



ISSN: 0067-2904

Automated Methodology for Volume Fraction Measurement of Three Phase Steel Micrograph Using Image Processing Techniques

Siddhartha Banerjee

Department of Computer Science, Ramakrishna Mission Residential College (Autonomous), Narendrapur,
West Bengal, India

Received: 21/4/2021

Accepted: 2/8/2021

Published: 30/10/2022

Abstract

A quantitative description of microstructure governs the characteristics of the material. Various heat and excellent treatments reveal micro-structures when the material is prepared. Depending on the microstructure, mechanical properties like hardness, ductility, strength, toughness, corrosion resistance, etc., also vary. Microstructures are characterized by morphological features like volume fraction of different phases, particle size, etc. Relative volume fractions of the phases must be known to correlate with the mechanical properties. In this work, using image processing techniques, an automated scheme was presented to calculate relative volume fractions of the phases, namely Ferrite, Martensite, and Bainite, present in the microscopic image of high strength low alloy steel. First, the microscopic image was segmented into Ferrite, Martensite, and Bainite regions. The phase structure's geometric property was used to identify different phases present inside the micrograph. After phase detection, the volume fraction of each region is calculated.

Keywords: Microstructure, phase, Image processing, Volume fraction.

1. Introduction

The properties of materials are governed by their micro-structure [1, 2]. Thus, it is essential to obtain a quantitative description of the micro-structure of the materials. This quantitative description can be achieved using direct and indirect approaches [3]. One indirect method example is X-ray diffraction-based measurement [4], where lattice parameters are measured to estimate structural parameters. On the other hand, in direct techniques, the structural parameters are directly measured.

Moreover, the presence of stress and texture may produce an erroneous result in an indirect approach. Microscopic investigations are performed in direct technique. In microscopic investigations, the metal surface is first observed using a microscope, and images of the observed surfaces are collected. Afterward, image processing and analysis techniques are applied to these microscopic images [5].

The microscopic images are called micro-graphs, which are first converted into digital form for subsequent storage, analysis, processing, and interpretation [6-10]. Digital Image processing techniques are widely used to extract specimen information from a micrograph. It has become an integral part of a microscopy-related experiments in metallurgy and materials engineering [11, 12].

*Email: sidd_01_02@yahoo.com

Segmentation is the most crucial step in the micro-graph analysis. The structure of the surface of investigated metal captured by microscopic image is called microstructure. Micro-structure consists of various phases denoting various phases. Features like gray level intensity, textural pattern, and edge orientation discriminate the different phases present in the micro-graph. The features will be used to discriminate between different phases depending on the material under study. Image processing techniques may be disturbed due to noise, impurities in the image acquisition system, or environmental issues (like contrast, brightness, magnification, etc.). These may pose additional challenges in the segmentation step. The similarity between the phase boundaries with one of the phases makes the task very difficult.

The most critical step in the quantitative analysis of the micro-graph is to classify different phases present in the dual-phase or multiphase metallography samples. The performance of the classification or segmentation of different phases tremendously influences the accuracy of subsequent measures. Researchers have applied different image processing techniques for this purpose, but the methodology has not been described in a structured manner. The methods depend on the manual application of different image processing techniques in an ad-hock manner. As a result, no general solution exists for micro-graph with different microstructures; it depends on the problem domain, which motivated us to focus on this problem.

In the present work, the task is to extract the three phases in steel and measure the volume fraction of these three different phases. Different phases in the micro-structures were formed due to various continuous cooling and isothermal heat treatments. Ferrite phases developed from the austenite phase if cooling was controlled. However, rapid cooling generates two phases – ferrite and martensite. Bainite was developed if the cooling process includes isothermal hold at some intermediate temperature. Bainite is the ferrite phase with retained austenite in it. The phases are observed at high resolution with Single Electron Microscope (SEM) micrograph, as shown in Figure 1.

Figure 1 consists of three phases: Ferrite, Bainite, and Martensite marked as F, B, and M, respectively. It can be observed from the micro-graph that martensite phases are smooth circular regions with high-intensity values. The remaining region inside and outside the circular martensite phase can be divided into two parts. The blackish portion with low intensity is the ferrite phase, and the portion with higher intensity within these ferrite phases is called the bainite phase. The work aims to classify these three phases in the micro-graph and separately identify the ferrite and bainite phases inside and outside the circular martensite phase. After correctly classifying the phases, the volume fraction of these phases is measured.

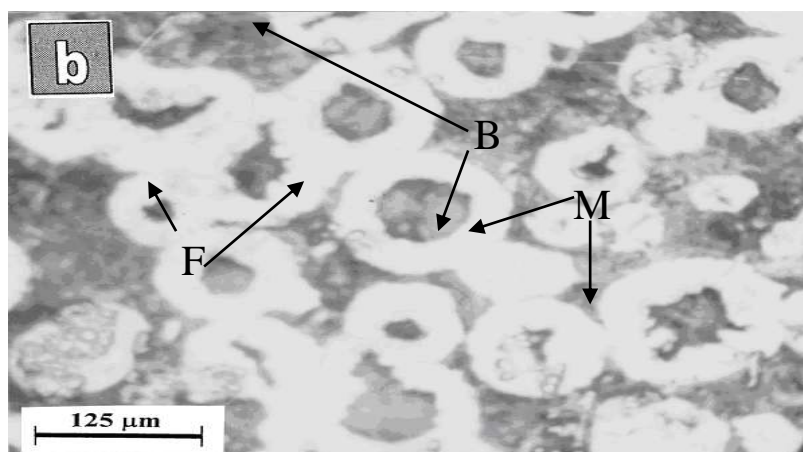


Figure 1: Three phases of metal

2. Past work

The quantification of phase volume fractions is commonly and almost routinely done using light microscopic images or scanning electron microscopic images of the microstructure. Before phase quantification, it is necessary to develop the material's micro-structure using small specimens metallographically polished and etched to develop the micro-structural details following standard metallographic procedure. It should be noted that the entire procedure of preparing the specimen is manual.

Microscopes were integrated with a digital camera, and the images captured by this camera were stored in a personal computer. The digital images of micro-structures were used for characterizing the micro-structure, including the relative volume fraction of the phases. The typical image analyzing software was generally used for this purpose. The microstructure analysis for the relative volume fraction of the phases was based on the grey level of different phases/constituents that developed depending upon the etching reagent and phase characteristics. However, only grey level-based analysis often poses difficulties in determining the phase volume fractions. This difficulty primarily arises from minimal variation in the grey level characteristics within/between the phases and in a complex structure where different phases with almost similar grey levels (or with no variation in grey level) remain finely intermixed. Hence, there remains challenging in such critical conditions to delineate different phases and determine the relative phase volume fraction. Keeping all these challenges in mind, the methodology for automated measurement mostly comes down to the task of image segmentation.

It is observed that very few efforts have been made to automate the segmentation of microstructures and measure the volume fraction of the phases present. Furthermore, the methodologies adopted are material specific. It is well known that the micro-structures vary from material to material and with different processing parameters. Hence devising an automated system applicable to all cases is very difficult. It has motivated the researchers to customize the systems for specific scenarios.

Komenda [13] proposed a scheme where an image classifier has been integrated with context vision [14]. Spatial dependencies between regions were measured to extract the areas of interest. However, such analysis incurs computational costs. Moreover, classification accuracy heavily depends on proper training. A neural network also has been tried to classify the phases of an alloy [15]. A comparative study has been done between multi-layer perceptron and self-organizing map topologies for segmenting micro-structures in metallographic images. In this work, a multi-layer perceptron neural network was trained using a supervised backpropagation algorithm, and self-organizing map neural network training was based on the unsupervised Kohonen algorithm. The network was trained using sixty samples of cast irons, and the results obtained by the multilayer perceptron neural network were very similar to the ones obtained by visual human inspection. It is worth mentioning that for such supervised techniques, sufficient samples are required for proper training. Chatterjee et al. [16] presented an image processing-based automated system that considered intensity-based thresholding to differentiate the phases in High Strength Low Alloy (HSLA) steel. To refine the measurement, phase boundaries with intensity values similar to one of the phases were identified as thin regions and ignored in the measurement. Gruttadauria et al. [17] utilized Image Pro Plus software to identify the phases, which also differentiated the phases based on intensity.

Paulic et al. [18] calculated graphite, ferrite, and ausferrite volume fraction using a threshold-based technique. Salem et al. [19] analyzed Ti6AlV4 microstructure data by learning the phase patterns. Campbell et al. [20] also worked with Ti6AlV4 specimens. Watershed transform followed by a merging technique had been used for region segmentation. In each region, phases were identified by using thresholding. Deep learning has been tried by Azimi et al. [21]. However, it requires a large data repository for formal learning. Gray-level co-occurrence-based textural properties were considered by Naik et al. [22] for phase identification. Yang et al. [23] quantify alpha and beta phases in dual-phase Ti-6Al-4V titanium using Image-Pro Plus software.

Commercially available software mainly relies on intensity-based thresholding, and the user provides an option to select the threshold. However, the brief discussion reveals that the problem was not that trivial. The threshold-based scheme fails to consider phase intensity variation and other structural criteria. Consequently, a more rigorous segmentation scheme becomes essential.

3. Methodology

The micrograph consists of three phases, as shown in Figure 2(a). Boundaries separated the phase regions in a micrograph. Sample Ferrite, Bainite, and Martensite region have been marked as F, B, and M, respectively, in Figure 2(a). As discussed earlier, the present work aims to classify the three phases in the micrograph and separately identify the ferrite and bainite phases inside and outside the circular martensite phase. The following significant steps were performed to achieve that.

1. Binarization of image
2. Detection of Martensite phase
3. Refinement of black regions
4. Classification of black regions
 - 4.1 Detection of the black region inside or outside of the Martensite phase
 - 4.2 Classification of Bainite and Ferrite phase

3.1 Binarization of the image

The gray-scale fractography image was first binarized using intensity-based thresholding. It has been discussed that, in general, the Martensite phase poses a higher intensity value, and the bainite and ferrite phases were characterized by low-intensity pixels. Using OTSU method of thresholding based on the intensity histogram, a threshold, this chosen so that $B[i, j] = 1$ if $F[i, j] > th$ and $B[i, j] = 0$ otherwise. $F[i, j]$ and $B[i, j]$ denote the pixel at $[i, j]$ location of the grayscale image and the corresponding image after binarization. The binarized image of the original micro-graph (Figure 2(a)) is shown in Figure 2(b).

3.2 Detection of martensite phases

After thresholding, the white region of the micro-graph was identified as the Martensite phase. The next task was to separate the bainite and ferrite phases from the black region.

3.3 Refinement of black regions

The bainite and ferrite phase was characterized by low-intensity value, but some white blocks may present in them. Hence, the bainite and ferrite phases were turned into a black region after thresholding. However, white blocks sometimes divide a black region into smaller subparts. Each black region was first marked by a unique number using a region-growing algorithm [24]. After that, erosion [25] operation was applied to join these smaller regions. However, after erosion, the area of the black region will increase. Hence, dilation was

applied [25] to remove the extra added areas.

After thresholding, some insignificant black regions may be present in the micro-graph due to noise. The following algorithm was used to remove the small insignificant regions.

Step 1: Calculate the size of each black region.

Step 2: Find the average sizes of the regions.

Step 3: If the black region's size is smaller than the average, remove the i -th region.

3.4 Classification of black regions

After preprocessing, the black regions were further classified into two phases: bainite and ferrite. Figure 2(a) shows that the ferrite phases were characterized by low intensity, whereas bainite phases were characterized by relatively high-intensity value but lower than the martensite phase. So local thresholding was applied to each black region using the OTSU method to classify the black regions into two phases. However, the two phases may be surrounded by the martensite phase, or the two phases may present in between two martensite phases. Hence, the bainite phases were separated inside and outside the martensite phase. The same was also done for the ferrite phase.

3.4.1 Detection of the black region inside or outside of the Ferrite phase

First, each black region's Centre of Gravity (COG) was calculated; then, finding a pixel in that region that is furthest from COG and calculating the Euclidian Distance (d) of that pixel from COG; then, drawing a circle considering COG as the center and d as the radius. If the circle covers more than one black region, it is considered a black region outside a ferrite phase; otherwise, it is considered inside the ferrite phase.

3.4.2 Classification of Bainite and Ferrite phase

Each black region inside or outside of Martensite phases was further classified as Bainite and Ferrite phases depending on local thresholding using the OTSU method. For this, a threshold is chosen depending on the intensity values of the original micrographs pixels in the black regions of the refined image. If the intensity of a fractography pixel in the black region inside the Martensite phase is less than *the*, then it can be characterized by the Ferrite phase inside the Martensite phase; otherwise, it is the Bainite phase inside the Martensite phase. The same method was applied for the black region outside the Martensite phase to classify it into Bainite and Ferrite phases outside the Martensite phases. The segmented image is shown in Figure 2(c), where the white regions correspond to the Martensite phase; blackish regions correspond to Bainite and Ferrite phase within the circular Martensite phase with two different shades, and the Bainite and Ferrite phase outside the circular Martensite phase was represented by a gray region with two different shades.

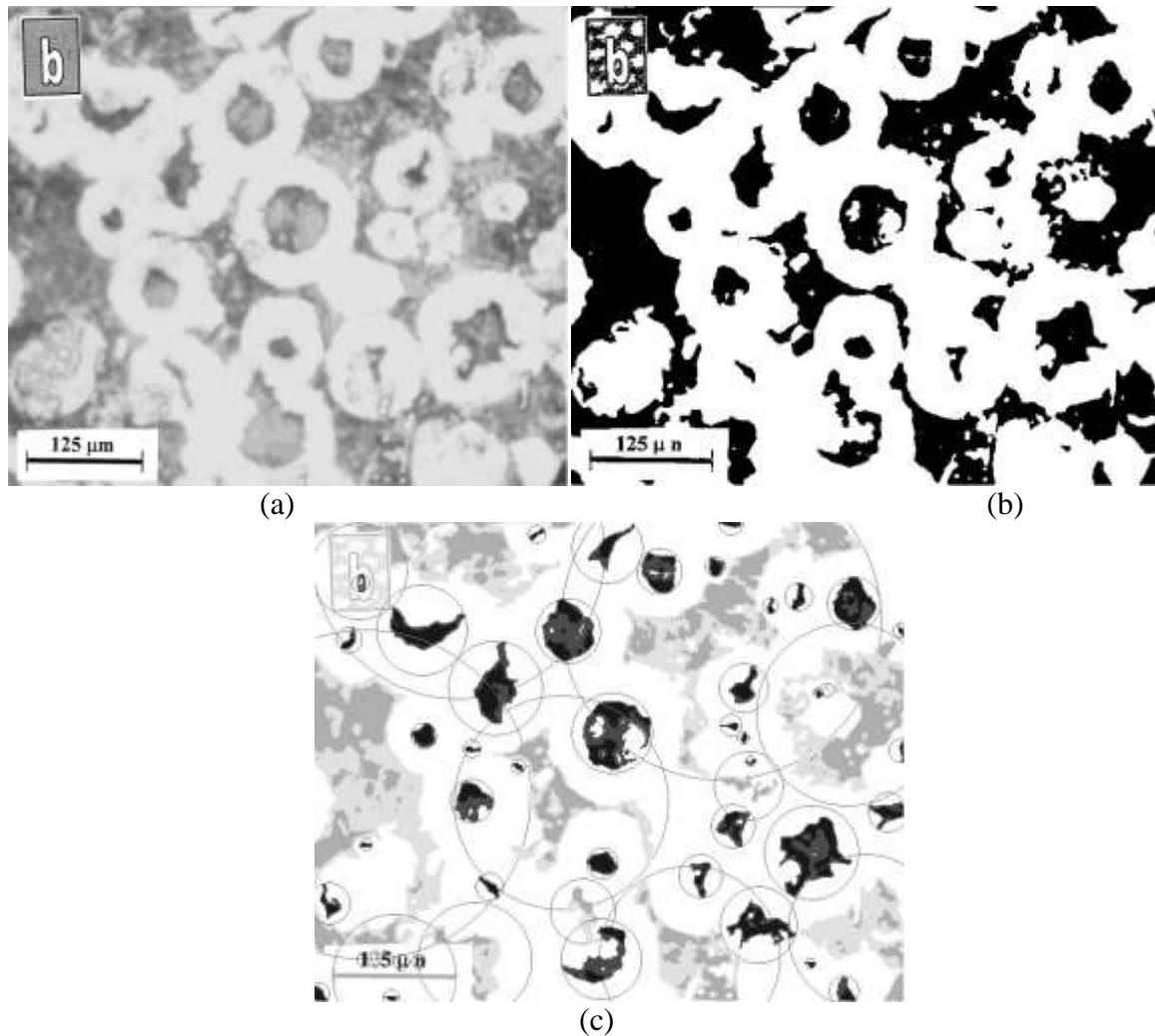


Figure 2: (a) Three Phase Micrograph (b) Threshold Image (c) Segmented Image.

Table 1: Volume Fraction of Different Phases

Micrograph	Martensite	Inside martensite		Outside martensite	
		Ferrite	Bainite	Ferrite	Bainite
Micrograph 1	.64	.03	.04	.12	.17
Micrograph 2	.65	.06	.06	.09	.14
Micrograph 3	.73	.04	.04	.09	.10
Micrograph 4	.65	.03	.05	.11	.16
Micrograph 5	.69	.04	.03	.11	.13

4. Results and Discussions

High Strength Low Alloy (HSLA) steel was used in the present investigation. The specimen was observed in a Scanning Electron Microscope (JSM6360) under secondary electron imaging mode, and the image was captured and stored in a computer. The brightness and contrast of the images were controlled by the in-built image controlling software of the microscope.

The proposed methodology was applied to 20 micrographs, and each micrograph's volume fraction of Martensite, Bainite, and Ferrite phases was calculated. The volume fractions for

five micrographs are listed in Table 1. It can be observed from the table circular martensite phase covers most of the area (60% to 75%) of the micrograph. The total ferrite phase inside and outside the circular martensite region covers more or less 15% of the total area. The bainite phase covers the remaining 15% to 20% area. The ferrite and bainite phase present inside and outside of the circular martensite phase are measured separately. It can also be observed from the result that the percentage of ferrite and bainite phases within the circular martensite phase was equally distributed. However, outside of the circular martensite phase, the occurrence of the bainite phase is slightly more than the ferrite phase. These observations can be used to control the material's properties.

Traditional commercially available software classifies the phases depending on intensity variation. Thus, this software can detect the volume fraction of the phases in the whole micrographs but cannot separately detect the volume fraction of bainite and ferrite phases inside and outside the circular martensite phase.

5. Conclusions

This work presents an automated scheme for extracting three phases, ferrite, martensite, and bainite, in high-strength low alloy steel. The scheme uses image processing operations like thresholding, region growing, erosion, and dilation to identify three phases. High-intensity circular-shaped Martensite phases were extracted using the Otsu thresholding method. The bainite and ferrite phases were spread inside and outside the circular martensite phase. The bainite and ferrite phases inside and outside circular martensite phases were determined separately using the geometrical property. At last, the volume fraction of different phases in the micrograph was measured. Most commercially available software classifies the phases based on intensity variation and fails to extract bainite and ferrite phases inside and outside the circular martensite phase separately.

References

- [1] N. J. Petch, "The cleavage strength of polycrystals," *Journal of the Iron and Steel Institute*, vol. 174, pp. 25–28, 1953.
- [2] W. L. Spychalski, K. J. Kurzydowski, and B. Ralph, "Computer study of inter- and intraangular surface cracks in brittle polycrystals," *Materials Characterization*, vol. 49, no.9, pp. 45–53, 2002.
- [3] T. Wejrzanowski, W. L. Spychalski, K. Rozniatowski, and K. J. Kurzydowski, "Image-based analysis of microstructures of engineering materials," *International Journal of Applied Mathematics and Computer Science*, vol. 18, no. 1, pp. 33–39, 2008.
- [4] C. E. Kril and R. Birringer, "Estimating grain-size distributions in nanocrystalline materials from x-ray diffraction profile analysis," *Philosophical Magazine A*, vol. 77, no. 3, pp. 621–640, 2001.
- [5] K. J. Kurzydowski and B. Ralph, *The Quantitative Description of the Microstructure of Materials*, CRC Press, London, 1995.
- [6] Q. Wu, F. S. Merchant, and K. R. Castleman, *Microscope Image Processing*, Academic Press, UK, 2008.
- [7] D. L. Spector and R. D. Goldman, *Basic Methods in Microscopy*, Cold Spring Harbor Laboratory Press, 2005.
- [8] G. Sluder and D. E. Wolf, *Digital Microscopy*, Academic Press, UK, 2003.
- [9] S. Inoue and K. R. Spring, *Video Microscopy*, Springer, 1997.
- [10] D. B. Murphy, *Fundamentals of Light Microscopy and Electronic Imaging*, Wiley-Liss, 2001.
- [11] K. R. Castleman, *Digital Image Processing*, Prentice-Hall, 1996.
- [12] A. Diaspro, *Confocal and Two-photon Microscopy*, Wiley-Liss, 2001.
- [13] J. Komenda, "Automatic recognition of complex microstructures using the Image Classifier," *Materials Characterization*, vol. 46, no. (2-3), pp. 87–92, 2001.
- [14] ContextVision AB, *Context vision Users's Guide, MicroGOP2000/S Software V. 3.1. ContextVision*, 1999.

- [15] V. H. C. de Albuquerque, A. R. de Alexandria, P. C. Cortez, and J. M. R. S. Tavares, "Evaluation of multilayer perceptron and self-organizing map neural network topologies applied on microstructure segmentation from metallographic images." *NDT & E International*, vol. 42, no. 7, pp. 644–651, 2009.
- [16] O. Chatterjee, K. Das, S. Dutta, S. Datta, and S. K. Saha, "Phase extraction and boundary removal in dual phase steel micrographs," *In Proceedings of India Conference (INDICON), IEEE*, 2010.
- [17] A. Gruttadauria, D. Mombelli, E. M. Castrodeza, and C. Mapelli, "Processing and characterization of dual phase steel foam," *Revista Materia*, vol. 15, no. 2, pp. 182–188, 2010.
- [18] M. Paulic, D. Mocnik, M. Ficko, J. Balic, T. Irgolic, and S. Klančnik, "Intelligent system for prediction of mechanical properties of material based on metallographic images," *Technical Gazette*, vol. 22, no. 6, pp. 1419–1424, 2015.
- [19] A. A. Salem, J. B. Shaffer, R. A. Kublik, L. A. Wuertemberg, and D. P. Satko, "Microstructure-Informed Cloud Computing for Interoperability of Materials Databases and Computational Models: Microtextured Regions in Ti Alloys," *Integrating Materials and Manufacturing Innovation*, vol. 6, no. 1, pp. 111–126, 2017.
- [20] A. Campbell, P. Murray, E. Yakushina, S. Marshall, and W. Ion, "New methods for automatic quantification of microstructural features using digital image processing," *Materials and Design*, vol. 141, pp. 395–406, 2018.
- [21] S. M. Azimi, D. Britz, M. Engstler, M. Fritz, and F. Mücklich, "Advanced Steel Microstructural Classification by Deep Learning Methods," *Scientific Reports*, vol. 8, 2018.
- [22] D. L. Naik, H. U. Sajid, and R. Kiran, "Texture-based metallurgical phase identification in structural steels: A supervised machine learning approach," *Metals*, vol. 9, no. 5, 2019.
- [23] D. Yang and Z. Liu, "Quantification of Microstructural Features and Prediction of Mechanical Properties of a Dual-Phase Ti-6Al-4V Alloy," *Materials*, vol. 9, 2016.
- [24] B. Chanda and D. D. Majumder, *Digital Image Processing and Analysis*, Prentice-Hall, India, 2001.
- [25] R. C. Gonzalez and R. E. Woods, *Digital Image Processing*, Prentice Hall, India, 1992.